Experiments on the wake flow behind different configurations of multirotor wind turbines

Experiments on the wake flow behind different configurations of multirotor wind turbines

Andreas Grodås Jørs[1], Torbjørn Lavik Mjåtveit[1], Morten Skoland[1], Gloria Stenfelt[1], Thomas Hansen[1], Jan Bartl[1]

[1] Dept. of Mech. and Marine Engineering, Høgskulen på Vestlandet (HVL), Bergen, Norway

E-mail: jan.bartl@hvl.no

Abstract. Multirotor wind turbine concepts have recently emerged as a promising alternative to conventional turbines. When arranged in farms, the wake flow behind multirotor assemblies becomes an important factor in the cost-of-energy equation. This paper presents a lab-scale experiment on the effect of rotor number, inter-rotor spacing and yaw-misalignment on the wake development behind a simplified multirotor model. The flow characteristics are investigated by towing different arrangements of porous discs in a large water tank while traversing an Acoustic Doppler Velocimeter in the wake. Results show lower initial velocity deficits in a multirotor's near wake, whereas its far wake is observed to be similar to the one of a single rotor. The wake's recovery rate is first stimulated by additional shear stresses in between the single rotors, while flattening off further downstream. Measurements on the wake flow behind individual yaw on the single rotors compared to collective yaw on all rotors show a similar deflection of the mean velocity deficit in the wake.

1. Introduction

We are currently observing large investments in the development of floating offshore wind in regions of deep waters around the world [1]. While current trends show steadily increasing rotor diameters, installing many smaller rotors on a single floating unit might be advantageous, especially when it comes to lower cost-of-energy related to simpler offshore installation and maintenance. This gave rise to multirotor concepts as an alternative to conventional large floating wind turbines. The use of less blade weight per total rotor swept area could be an additional factor for potential cost savings [2]. Despite these benefits, multirotor concepts provide us with some engineering challenges, such as designing for locally blocked rotors or finding a layout for a minimal downstream impact of a multirotor's wake flow.

One of the first studies on multirotor aerodynamics was presented by Chasapogiannis et al. [3]. Their computational study showed an increase of both power output and thrust force of a multirotor with seven rotors (MR7) compared to a single rotor, and identified local regions of increased flow velocities in the wake between the rotors. The influence of lateral rotor spacing on power and thrust was investigated by Martín San Román et al. [4]. Using free-wake vortex methods, they showed increasing power and thrust coefficients when the spacing between the rotors was decreased. Ghaisas et al. [5] performed a large-eddy simulation (LES) of the wake flow behind a multirotor consisting of four rotors (MR4). They showed a faster wake recovery for the MR4 than for a single rotor, although the investigated inter-rotor spacings were rather large. An extensive investigation of the performance and wake flow behind the Vestas demonstrator

MR4 multirotor turbine was presented by van der Laan et al. [6]. By the means of Reynolds-averaged Navier-Stokes (RANS) computations, a faster wake recovery of the MR4 compared to the wake of an equivalent single rotor was shown. This was furthermore confirmed by full-scale measurements on the 4 x 0.75 MW demonstrator turbine. Another comprehensive LES-study on the effects of rotor number, spacing and rotational direction was performed by Bastankhah and Abkar [7]. Their results gave detailed insight in wake recovery processes and also concluded that multirotor turbines could mitigate wake effects in farm arrangements. A number of interesting experiments on shrouded multirotor wind turbines were performed over the last few years in the wind tunnel at the Kyushu University in Japan by Göltenbott et al. [8] and Wantanabe et al. [9]. Both measured an increased power production for the central rotor in an multirotor arrangement compared to the neighboring rotors for different lateral turbine spacings.
The characteristics of wake flow behind multirotor wind turbines become specifically important when multirotor systems are arranged in farm layouts. Van der Laan and Abkar [10] discussed the benefit of the faster multirotor wake recovery for different inter-turbine spacings. The relative increase in a farm's annual energy production was larger for tighter spacings. These results were confirmed by Kirchner-Bossi and Porté-Agel [11], who additionally used optimisation methods for a farm arrangement of multirotor wind turbines. For the whole farm, they found total power improvements, most significant for small spacings between the multirotor systems and low inflow turbulence levels.
Using wake steering through intentional yaw misalignment of wind turbines has been widely discussed as an efficient method for wind farm control over the last couple of years [12], [13]. Given its potential, this control method could also be effective for farms of multirotors. However, yawing a multirotor arrangement is a challenge in itself. A variety of different methods have been proposed for different multirotor concepts. These include individual yaw of the single rotors or collective yaw by moving the whole frame [14]. The fact that a new degree of freedom is introduced by individual wake steering of multirotor wind turbines has recently been discussed in a LES-study by Speakman et al. [15]. By yawing the individual rotors of a MR4 setup, the authors show the potential to both, channelling and expanding a multirotor wake, which can have a considerable impact on both the distribution and magnitude of the velocity deficit. In a recent experimental wind tunnel study Xiong et al. [16] analysed the wake recovery process behind a MR4 setup in zero-yaw and a yaw angle of $\gamma = 10^o$. The wake deflection behind a multirotor with individually yawed turbines was observed to be larger than behind a yawed single rotor, especially for larger downstream distances in the far wake.
In this paper, we present measurements of the wake flow behind simplified, porous discs in a single rotor (SR), MR4 and MR7 arrangement. We investigate the influence of rotor number, inter-rotor spacing and individual and collective rotor yaw on the mean and turbulent wake flow. The yawed experiments are conducted on a MR7 arrangement with constant inter-rotor spacing of s/d= 0.1, where s is the spacing between two adjacent rotors of diameter d.
The paper at first gives an overview over the experimental models, their setup and instrumentation used. Thereafter, results on the influence of rotor number, inter-rotor spacing and individual and collective yaw misalignment are presented and discussed.

2. Methods

2.1. Multirotor models

The multirotor models are assembled using four to seven porous discs, with radially increasing porosity. The laser-cut aluminum discs have a diameter of $d = 200$ mm and thickness of $t = 5$ mm. The solidity of each disc is $\sigma = 57\%$, which results in a measured thrust coefficient of $C_T = 0.95$ for each individual disc. The discs' design is similar to the actuator discs used in previous wake flow experiments by Camp and Cal [17], Helvig de Jong et al. [18] or Neunaber et al. [19]. Figure 1 shows the three baseline setups of the discs: a single rotor disc (SR), an

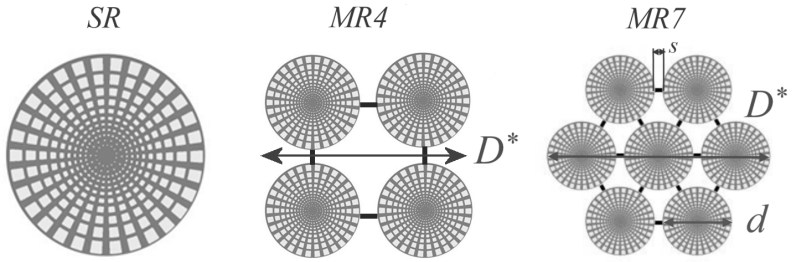

Figure 1. Experiment 1: Single rotor disc (SR), multirotor of four discs (MR4) and multirotor of seven discs (MR7). d is a disc's diameter; s is the inter-rotor spacing; D^* is the multirotors' edge to edge diameter.

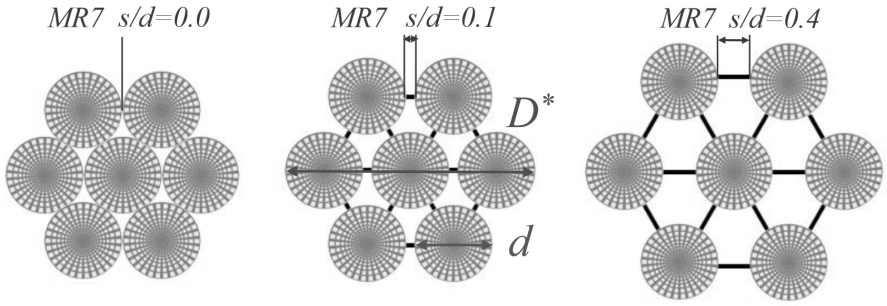

Figure 2. Experiment 2: Hexagonal arrangement of multirotors of seven discs (MR7). The inter-rotor spacing is varied between s/d=0.0, 0.1 and 0.4. d is a disc's diameter; s is the inter-rotor spacing; D^* is the multirotors' edge to edge diameter.

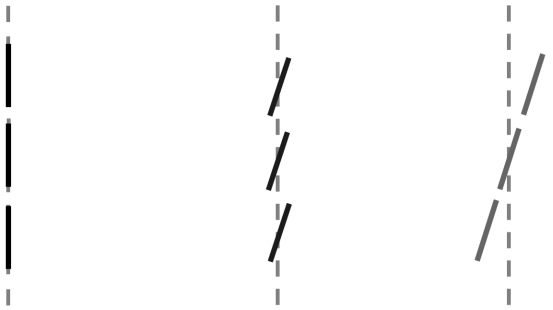

Figure 3. Experiment 3: Top view on multirotors of seven discs (MR7) in different yaw configurations. Zero yaw, $\gamma = 0^o$ (left panel), individual yaw, $\gamma = 10^o$ (middle panel) and collective yaw, $\gamma = 10^o$ (right panel).

arrangement of four discs (MR4) and another one of seven discs (MR7). The discs are connected via a quadratic (MR4) or a hexagonal (MR7) support structure, made of of cylindrical rods of diameter $d_{\text{support}} = 10$ mm connecting the disc centers. As shown in Figure 5 the center of the multirotor setups is located at a depth of $z_C = -1000$ mm and is connected to a tower of diameter $d_{\text{tower}} = 20$ mm with a total submerged length of $h = 1000$ mm. In Figure 2, arrangements of the MR7 multirotor with increasing inter-rotor spacing from $s/d = 0.0$, 0.1 and 0.4 are depicted. In Figure 3, a top view of the MR7 setup in three different yaw configurations is sketched. A non-yawed reference case is compared to a yawed case with individually yawed discs and a collectively yawed multirotor. In all cases the inter-rotor spacing is kept $s/d = 0.1$.

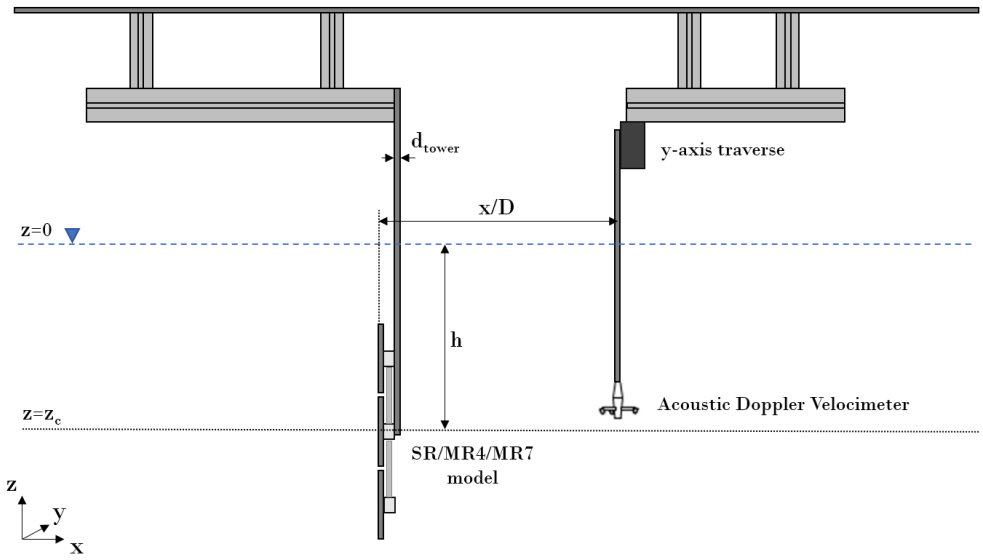

Figure 4. Sketch of measurement setup in the towing tank. Two towing carriages connected through a wire are shown, one carrying the multirotor, the other carrying the ADV traverse.

2.2. Velocity measurement in the towing tank

The presented experiments are performed in the MarinLab towing tank at the Western Norway University of Applied Sciences (HVL). The towing tank is 50 m long, 3.0 m wide and 2.2 m deep. Reynolds-scaling at low velocities enables to perform stationary aerodynamic experiments in water. Experiments on scaled wind turbine rotors have previously been performed in towing tanks by Barber et al. [20] and Kress et al. [21].

The towing velocity in these experiments is set to $u_0 = 0.50$ m/s, while the velocity in the wake is measured by a Nortek *Vectrino+* Acoustic Doppler Velocimeter (ADV). A rather low towing speed is used to prevent wave production in the wake, which could potentially disturb the near surface flow. The three-dimensional velocity vector in the wake is measured with the ADV at 200 Hz. A more detailed description of the measurement principles is given in Bartl et al. [22]. The Reynolds number based on a single disc's diameter is $Re_d \approx 10^5$. Figure 4 shows a sketch of the measurement setup in the towing tank. The multirotor model is mounted on a front towing carriage, while the ADV is mounted on to an automated traverse on a second carriage. The carriages are connected with a steel wire. The axial distance x/D in x-direction between them can be varied. The automated traverse allows a horizontal (y-direction) movement of the ADV measurement device.

2.3. Measurement locations

Wake flow measurements are carried out in the wake of the different multirotor arrangements. The wake flow is measured at four downstream locations, $x/D = 2$, 4, 7 and 10 at the center depth behind the turbines as displayed in Figure 5. Additional point measurements are recorded along the centerline perpendicular to the disc in the streamwise direction for the multirotors, which extends from $x/D = 1$ to 10. In this way, the streamwise development of velocity deficit and turbulent kinetic energy can be compared for the different setups. The reference diameter D used for quantifying the downstream distances x/D in the wake is chosen to be $D_{\mathrm{MR4}} = 2d$ and $D_{\mathrm{MR7}} = 3d$. Thus, this definition is independent of rotor spacing, but disregards the fact that the total multirotor diameter $D^*_{\mathrm{MR4}} = 2d + s$ and $D^*_{\mathrm{MR7}} = 3d + 2s$, respectively, is actually larger. A follow-up paper will further discuss the use of different reference diameters.

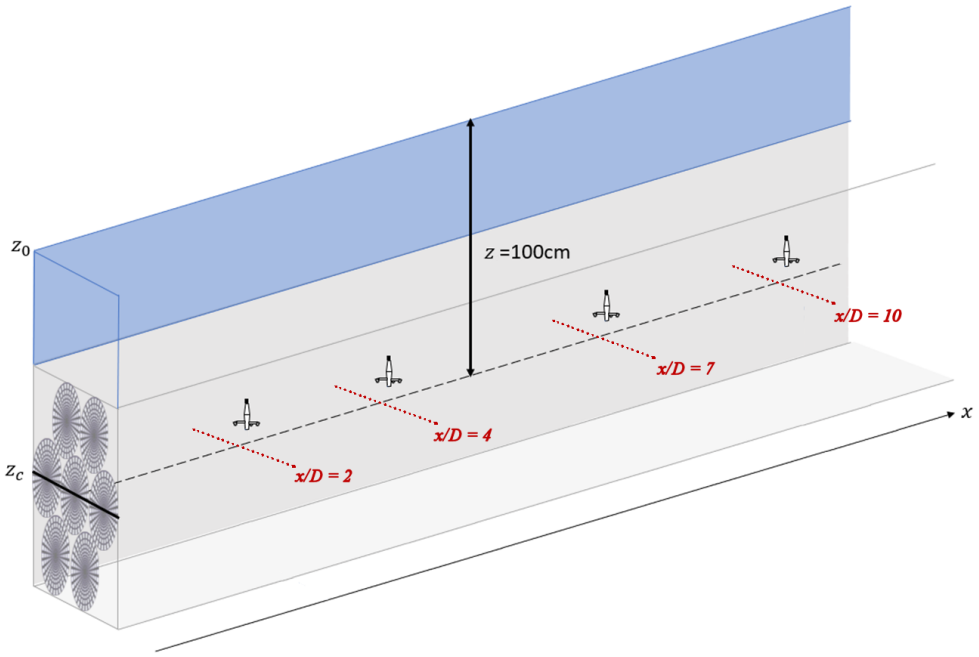

Figure 5. Measurement locations in the wake at $x/D = 2$, 4, 7 and 10 downstream of the multirotor setup. For the MR4 setup the reference diameter is $D_{\mathrm{MR4}} = 2d$, while for the MR7 it is $D_{\mathrm{MR7}} = 3d$.

3. Results

In this section the transverse and streamwise velocity profiles measured in the wake are presented as experiments 1, 2 and 3. Hence, in the first sub-section the influence of the rotor number on the wake is analysed. The second sub-section investigates the influence of the inter-rotor spacing s/d on the wake development. Finally, in the third sub-section, the influence of yaw misalignment is studied. For all results, the average velocity deficit u is normalised with the freestream velocity u_0, and the cross-sectional position y is divided by the diameter D and D^*, respectively, of each rotor setup. The turbulent kinetic energy tke is calculated with equation (1) and later normalised with the squared freestream velocity u_0^2.

$$tke = \frac{1}{2}[(u')^2 + (v')^2 + (w')^2] \tag{1}$$

3.1. Experiment 1: Influence of rotor number

A comparison of the cross-sectional wake profiles for the three different rotor setups are presented in Figure 6 with an inter-rotor spacing of $s/d = 0.1$ for MR4 and MR7. Velocity profiles are measured at downstream distances $x/D = 2$, 4, 7 and 10. The vertical lines indicate the individual rotors of the different setups. At $x/D = 2$ both multirotors have an equally low velocity deficit compared to the single rotor, recovering to around 70% of the freestrem velocity. This might be due to jet streams between the discs, leading to higher shear stresses in the near wake. MR4 shows a lower velocity drop at the middle of the rotor as opposed to the single rotor and MR7, which is most likely due to the center opening. While MR4 may experience jet streams in the middle, the single rotor and MR7 have a disc blocking the flow at the center. Note that a slightly negative velocity is measured in the wake center behind the single rotor here, indicating reversed flow. This is likely due to the high local solidity of the disc model in its center. Here, in the near wake, significant differences in the wake characteristics of discs and

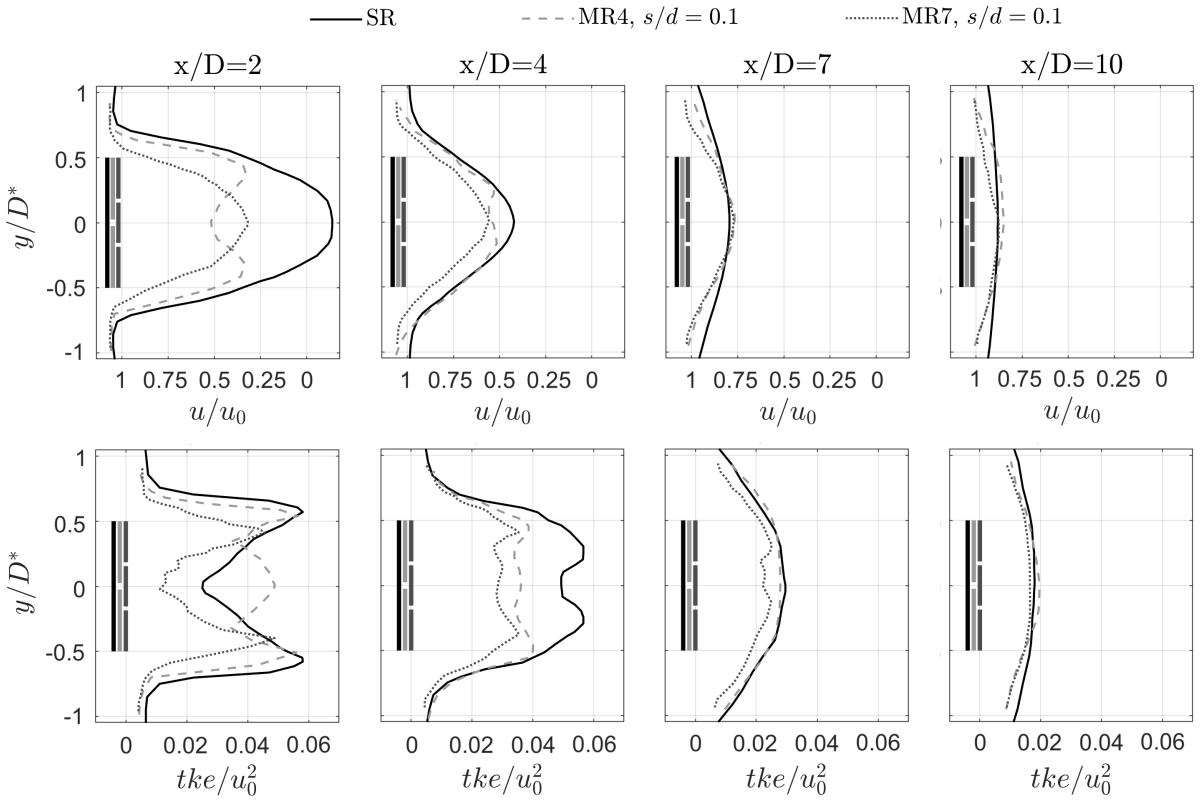

Figure 6. Normalised mean velocity deficit u/u_0 (upper row) and normalised turbulent kinetic energy tke/u_0^2 (lower row) measured at four downstream distances $x/D = 2$, 4, 7 and 10. Profiles are compared for a single rotor (SR), multirotor 4 (MR4) and multirotor 7 (MR7), with an inter-rotor spacing of $s/d = 0.1$ each.

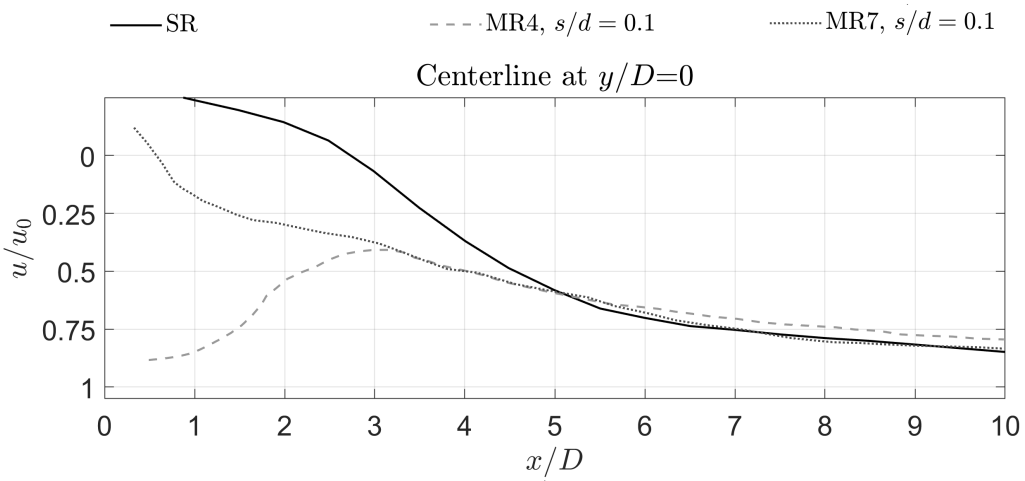

Figure 7. Normalised mean velocity deficit u/u_0 measured at the centerline $y/D = 0$ behind a single rotor (SR), multirotor 4 (MR4) and multirotor 7 (MR7).

rotors are present as previously discussed by Helvig et al. [18]. Further downstream, at $x/D = 4$ all wakes develop into a Gaussian shape. MR7 has regenerated slightly more than MR4 at 45% and 50% of the inflow velocity, respectively. Although the single rotor is still at 60%, it recovered 40% of its deficit within an axial distance of only two diameters. This could be explained by higher turbulent mixing at $x/D = 2$ and 4 than for the compared multirotors. Turbulent mixing is driven by local shear stresses which are likey to be higher at these locations. It is also worth noting that all curves have a more uniform shape, proving that the wakes are well mixed at this downstream distance. At $x/D = 10$ the wake profiles are more similar. The single rotor wake has recovered the most, having a velocity deficit of 15% compared to both multirotors being at 20%. Their shapes are all similar and more widespread, with no distinct peaks. This is due to the wake expansion driven by mixing with freestream flow in the regions at $y/D^* = \pm 0.5$. The velocity deficits are therefore more evenly distributed along the cross-section. Overall, the major differences between the setups can be found in the near wake, where the geometry plays a key role for rotor-added turbulence, shear stresses and streamwiese velocity deficit.

In Figure 7, a continuous wake development is presented at downstream distances ranging from $x/D = 1$ to 10. The data was recorded by a streamwise traverse of the ADV along the centerline at $y/D = 0$. In the wake of the rotor setups some distinct differences are observed. All curves seem to meet at around $x/D = 5$ even though they have different paths. While the wake behind the single rotor and MR7 have a high initial velocity deficit in the center, MR4 wake is observed to have a much larger velocity in the near wake. This is most likely because of its opening in the turbine center, where a jet of high velocity is flowing through the MR4 setup. For the MR7 setup, the most significant velocity decrease is observed right behind the rotor, evening out for larger downstream distances. In contrast to that, the single rotor wake deficit initially decreases much slower and reaches an inflection point at roughly $x/D = 2.5$. At a similar downstream distance, the wake behind the MR4 has a global maximum, most likely due to the individual discs wakes merging into one larger wake at around this location. After $x/D = 5$ the velocity regeneration follows a rather similar path for all disc setups.

3.2. Experiment 2: Influence of inter-rotor spacing

Various MR7 setups were studied in this section to be able to quantify effects of inter-rotor spacing on the wake development. Wake profiles for MR7 are measured for three different inter-rotor spacings, $s/d = 0.0$, 0.1 and 0.4, respectively. The results are presented in Figure 8. A significant variation in the wake for the different setups at $x/D = 2$ downstream is observed. The configuration featuring a spacing of $s/d = 0.4$ has the lowest velocity deficit of approximately 40% at this location. In contrast, the $s/d = 0.0$ setup has barely regained any velocity, while the wake behind the $s/d = 0.1$ setup peaks at about 70% of the freestream velocity. These observations indicate that larger inter-rotor spacing could lead to smaller velocity deficits in the near wake region. At a downstream distance of $x/D = 4$, however, the velocity deficits between all three setups are seen to be very similar. The $s/d = 0.4$ setup still has the lowest velocity deficit, with the setup featuring spacings of $s/d = 0.0$ and 0.1 being not far apart. The rate of velocity recovery might therefore actually be larger for smaller inter-rotor spacing from this location and downstream. In the far wake region, from $x/D = 7$-10, the the three wake profiles are at an almost equal level. The wake profile for the multirotor with $s/d = 0.0$ spacing is observed to develop similar to a single rotor wake. Small jet streams in the triangular spaces between the individual discs are deemed to be the reason for the observed difference.

In Figure 9 the centerline velocity deficit is compared between the three MR7 setups with different inter-rotor spacings. The setup with $s/d = 0.4$ spacing shows a high level of velocity deficit behind the turbine, which flattens out at a downstream distance of $x/D \approx 2$. When comparing the setup with $s/d = 0.0$ and $s/d = 0.1$, the latter recovers faster between $x/D = 1$ and $x/D = 3$. This may be caused by the larger jets between the discs. The wake development

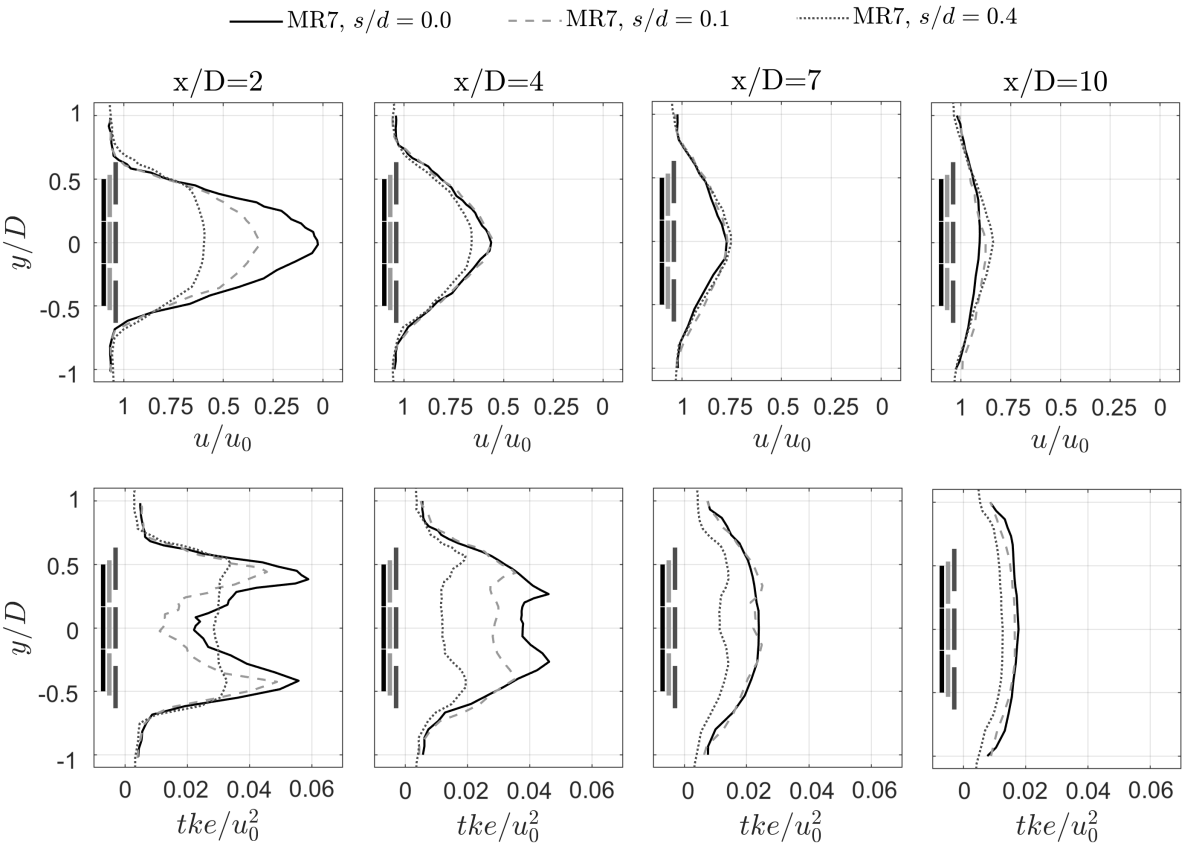

Figure 8. Normalised mean velocity deficit u/u_0 (upper row) and normalised turbulent kinetic energy tke/u_0^2 (lower row) measured at four downstream distances $x/D = 2$, 4, 7 and 10. Profiles are compared for a multirotor 7 (MR7), with an inter-rotor spacing of $s/d = 0.0$, 0.1 and 0.4.

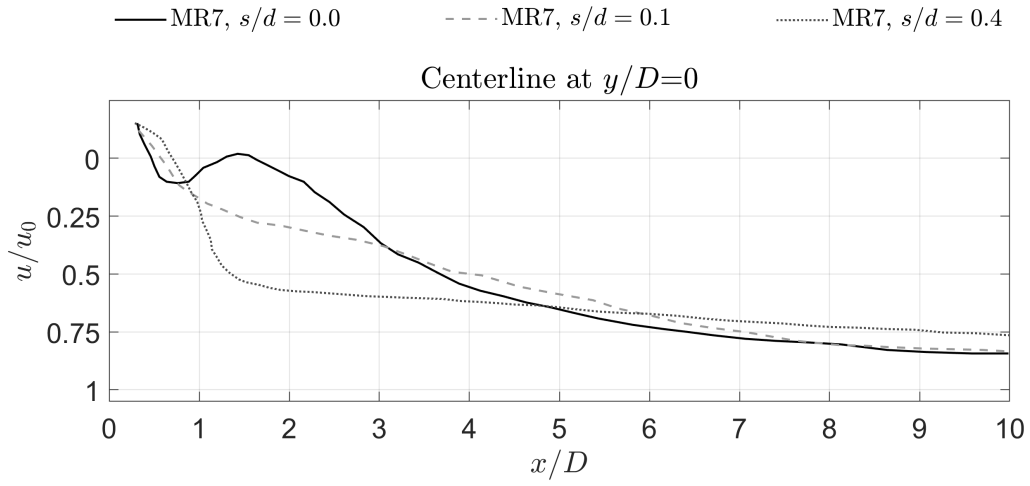

Figure 9. Normalised mean velocity deficit u/u_0 measured at centerline y/D=0 behind a multirotor 7 (MR7) with different inter-rotor spacings s/d=0.0, 0.1 and 0.4.

behind the $s/d = 0.0$ setup shows a second peak at $x/D = 1.5$, delaying the recovery in this region. However, at $x/D = 3$, the two curves meet again. After $x/D = 4$ only smaller differences in the velocity deficit for the three configurations are observed. At a downstream distance of $x/D = 10$, the wake velocities behind the three setups have recovered to about 75-80% of the incoming velocity. When comparing the MR7 with $s/d = 0.0$ spacing against the single rotor (Figures 7 and 9), the multirotor's wake development is very similar to the single rotor's wake. Velocity deficit and turbulent kinetic energy follow a similar path for both configurations. Small differences are observed in the very near wake from $x/D = 0.5$ to $x/D = 1.5$, where jet flows through the small spaces in between the rotor-discs of the multirotors leave their footprint. In other words, a very tightly spaced multirotor could almost be regarded as a single disc with six extra triangular spaces (see Figure 2).

3.3. Experiment 3: Influence of yaw misalignment

To align the individual rotors in a multirotor arrangement with the incoming wind is not as obvious as for a single wind turbine. The various multirotor concepts are considering different yawing mechanisms, while either the individual rotors are yawed or all rotors are collectively yawed by moving the entire frame. Figure 10 shows a comparison of the velocity deficit and turbulent kinetic energy measured behind these two setups for a yaw angle of $\gamma = 10^o$. It is observed that the wake is deflected for both individual yaw and collective yaw. Both concepts result in a similar deflection towards positive y-values, while the magnitude of the velocity deficit is similar to the zero-yaw reference case. Similar conclusions can be drawn for the turbulent kinetic energy in the yawed wake configurations, while only minor differences in the peak turbulence are observed. However, these observations are only valid for the wake flow measured in the near wake at a downstream distance of $x/D = 2$, and further downstream distances should be investigated in future studies to be able to assess the full potential for wake steering behind multirotors. Comparing the deflected wake to results by Xiong et al. [16], similar magnitudes in wake deflection at $x/D = 2$ can be stated. Significant differences are, however, observed due to the single peak wake profile behind an MR7 arrangement compared to the double peaked velocity deficit behind an MR4 setup.

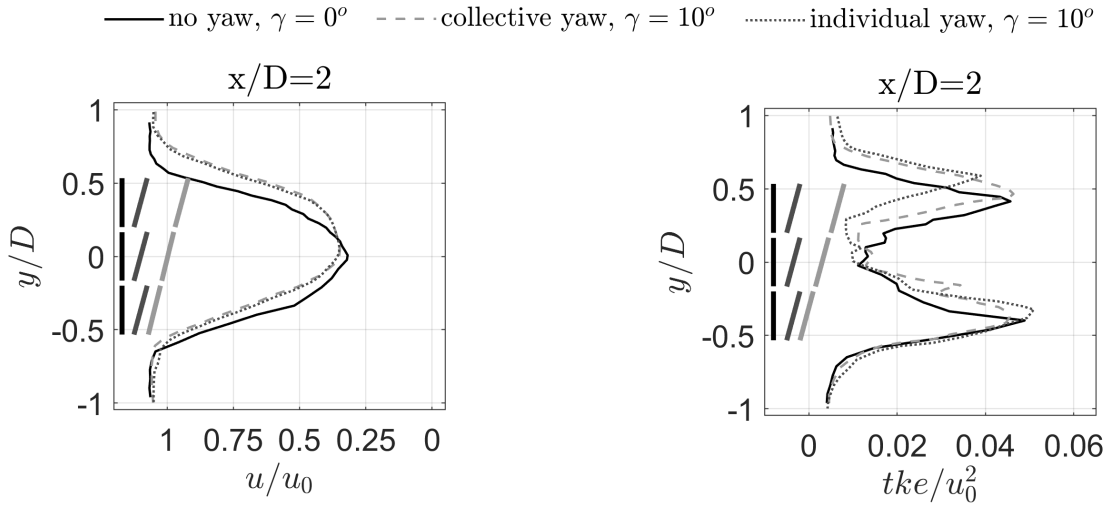

Figure 10. Normalised mean velocity deficit u/u_0 (left) and normalised turbulent kinetic energy tke/u_0^2 (right) behind a MR7, $s/d = 0.1$ measured at downstream distance $x/D = 2$. Profiles of two different yaw configurations with $\gamma = 10^o$ are compared to the zero yaw reference case.

4. Conclusions

Preliminary results show that a multirotor wake has lower initial velocity deficits in the near wake than a single rotor. Furthermore, rotor-generated turbulence levels behind multirotor arrangements are observed to be lower than for a single rotor. Further downstream, however, the multirotor wake recovers at a slower rate than the single rotor wake. Consequently, a multirotor's far wake at $x/D = 10$ is seen to have similar velocity deficits compared to a single rotor. When discussing wake recovery of a multirotor, it is important to specify whether the total multirotor diameter or the sum of the individual rotors of a multirotor is used as a reference. An increase in the disc spacing in the multirotor system is found to decrease the initial velocity deficit and turbulence produced in the wake. However, compared to the setup's increased total diameter, a larger disc spacing shows a faster wake recovery in the far wake. The various concepts of multirotors are considering different yawing mechanisms, where either the individual rotors are yawed or all rotors are collectively yawed by moving the entire frame. It is observed that the wake is deflected for both individual yaw and collective yaw. Both concepts result in approximately the same deflection in the near wake, while the magnitude of the velocity deficit is similar to the zero-yaw reference case.

Our results indicate the potential for closer turbine spacing in multirotor wind farms compared to single rotor farms, and thus confirm previous results by van der Laan and Abkar [10] and Bastankhah and Abkar [7]. A higher number of rotors was observed to have advantageous effects on wake recovery. The choice of an appropriate inter-rotor spacing in a future multirotor design is deemed to be an optimisation problem. While our results show benefits of large inter-rotor spacing for faster wake recovery, smaller spacings will most likely increase the energy extraction per total area and decrease material use and weight. Furthermore, wake steering by yaw is deemed to be an effective tool for wind farm control also in potential future multirotor farms. However, our preliminary results can only serve as a proof-of-concept at this stage, while future experiments at larger downstream distances and a greater variety of individual yaw angles similar to cases defined by Speakman et al. [15] should be further investigated.

References

[1] Bento N and Fontes M 2019 *Renew Sust Energ Rev* **99** 66–82
[2] Jamieson P and Branney M 2012 *Energy Proced* **24** 52–59
[3] Chasapogiannis P, Prospathopoulos J, Voutsinas S and Chaviaropoulos T 2014 *J Phys Conf Ser* **524** 012084
[4] Martín San Román R, Benito-Cia P, Azcona J and Cuerva A 2022 *J Phys Conf Ser* **2362** 012024
[5] Ghaisas N, Ghate A and Lele S 2018 *J Phys Conf Ser* **1037** 07202
[6] vdLaan P, Andersen S, García N, Angelou N, Pirrung G, Ott S, Sjöholm M, Sørensen K, Neto J, Kelly M, Mikkelsen T and Larsen G 2019 *Wind Energ Sci* **4** 251–271
[7] Bastankhah M and Abkar M 2019 *Phys Fluids* **31(8)** 085106
[8] Göltenbott U, Ohya Y, Yoshida S and Jamieson P 2017 *Renew Energ* **112** 25–34
[9] Watanabe K and Ohya Y 2019 *J Energ Resour-ASME* **141** 051211
[10] vdLaan P and Abkar M 2019 *J Phys Conf Ser* **1256** 012011
[11] Kirchner-Bossi N and Porté-Agel F 2020 *J Phys Conf Ser* **1618** 032014
[12] Gebraad P, Thomas J, Ning A, Fleming P and Dykes K 2017 *Wind Energ* **20(1)** 97–107
[13] Bartl J, Mühle F and Sætran L 2018 *Wind Energ Sci* **3** 489–502
[14] Störtenbecker S, Dalhoff P, Tamang M and Anselm R 2020 *Wind Energ Sci, 2020* **5** 1121–1128
[15] Speakman G, Abkar M, Martínez-Tossas L and Bastankhah M 2021 *Wind Energ* **24(11)** 1294–1314
[16] Xiong X, Laima S and Li H 2023 *Ocean Eng* **269** 113594
[17] Camp E and Cal R 2016 *Phys Rev Fluid* **1** 044404
[18] Helvig S d J, Vinnes M K, Segalini A, Worth N A and Hearst R J 2021 *J Wind Eng Ind Aerod* **209** 104485
[19] Neunaber I, Hölling M, Whale J and Peinke J 2021 *Renew Energ* **179** 1650–1662
[20] Barber S, Wang Y, Jafari S, Chokani N and Abhari R 2011 *J Sol Energy Eng* **133** 011007
[21] Kress C, Chokani N and Abhari R 2016 *Renew Energ* **89** 543–551
[22] Bartl J, Aasnæs C, Bjørnsen J, Stenfelt G and Lande-Sudall D 2022 *J Phys Conf Ser* **2362** 012004